# IMPLEMENTATION OF VECTOR CONTROL FOR GRID VOLTAGE SUPPORT IN VSC-HVDC TRANSMISSION SYSTEM

**Ahmed F. Abouzeid, Ahmed A. Daoud and Sobhy S. Dessouky**
Electrical Power Engineering
Port-Said University, Port Said, Egypt, 42523
Ahmed_Abouzeid@eng.psu.edu.eg

**Juan M. Guerrero**
Dept. of Elect. Computer & System Engineering
University of Oviedo, Gijon, Spain, 33204
guerrero@uniovi.es

***Abstract:*** *This paper presents a performance study of voltage source converter high-voltage direct-current (VSC-HVDC) transmission system for supporting grid voltage under different operating conditions. The VSC-HVDC transmission system is used to integrate an off-shore wind power plant to grid. The vector control method is used to make a decoupled control of active and reactive powers for grid voltage disturbances mitigation. The dynamic behavior of the system is evaluated using MATLAB/SIMULINK package. Finally, the control method of the system integration into a small-scale grid side converter connected to a virtual-grid using the TMS320F28335 from Texas Instruments has been implemented. The simulation and experimental results were matched showing a good performance under different operating conditions.*

***Key words:*** *HVDC transmission; vector control; off-shore wind power; grid integration; voltage-source converter.*

## 1. Introduction

The recent decades have seen increased demand for reliable and clean forms of energy instead of conventional energy sources. Wind energy has shown the fastest rate of growth among different renewable energy sources that will reach to 666.1 GW of the cumulative worldwide capacity by 2019 (GWEC report, 2014) [1]. While, wind energy has some disadvantages such as the variation of the generated power for different locations and seasons due to the nature of the wind profile. Besides, good wind sites are often located far from cities in remote locations implying more cost, some impact on the environment because of the noise produced by the rotor blade and visual impact. Off-shore wind turbines overcome those drawbacks since the wind profile is uniform and far from the land. Consequently, future wind farms will be off-shore several hundred kilometers between the wind farm and the grid connection point.

High voltage direct current (HVDC) transmission may be the only feasible option for transmitting bulk power over long distances of more than 50 km with lower electrical losses than high voltage alternating current (HVAC). HVDC transmission systems have been built using two converter types: current source converter (CSC-HVDC), which uses line-commutated switching devices (thyristors) or voltage source converter (VSC-HVDC), which uses self-commutated switching devices such as IGBT, MOSFET, and GTO. Various HVDC configurations are summarized in [2-5] depending on the function and location of the converter station.

Electrical grid network comprises of different elements like generators, transmission lines and loads. Many disturbances could be occurred per a day to the grid network such as losing number of generators, transmission lines and/or loads variations. As a result, the grid voltage could be varied (increase/decrease) depends on the type of disturbance that might cause mal-operation or disconnection of other loads connected to the same grid. Therefore, the presence of a device that can generate/absorb reactive power at the grid terminal would help on mitigation of the grid voltage disturbances occurred.

In this paper, besides of being transmitting active power from the off-shore wind power plants, the on-shore side converter is used to compensate the reactive power needed for the voltage disturbance mitigation using vector control.

## 2. System description

Fig. 1 shows the proposed VSC-HVDC system that connects an off-shore wind power plant (WPP) of 300 MW rating to the main grid through a 100 Km HVDC transmission cables. The WPP (sending side) is aggregated and modelled as an ac source assuming that wind turbines are perfectly controlled to capture the maximum power from the wind. System parameters are given in table 1 in the appendix.

- The phase reactor acts as a filter for the harmonic content produced by the converter switching. The main purpose of the reactor is to avoid a short circuit between the inverter and the grid. It also provides an independent control of active and reactive power by controlling the voltage drop and the current direction across it.
- A 350 MVA Delta/grounded-wye transformer is used to eliminate the third harmonic current generated by the converter.

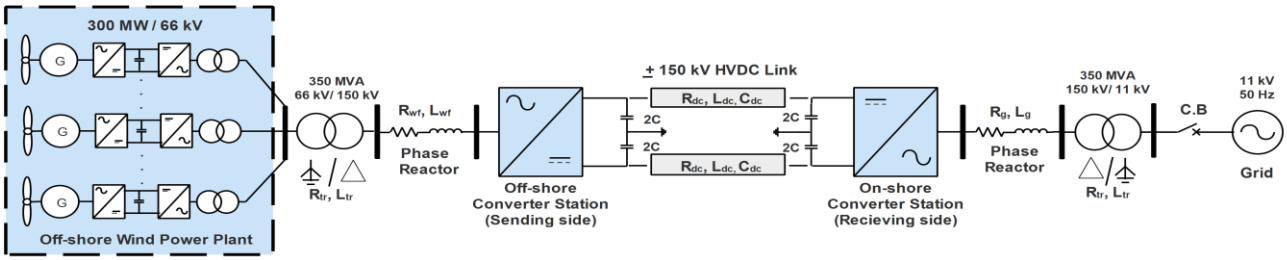


Fig. 1 Schematic diagram of offshore wind power plant grid integration via VSC-HVDC.

In addition, the transformer maintains an effectively grounded system even when the distributed generation becomes islanded [6].

• Both on-shore and off-shore converter stations are two-level VSC using several modules of power semiconductors each comprising an IGBT with anti-parallel free-wheeling diodes. These two components are integrated in the same semiconductor package to provide current capability in the reverse direction and to prevent the application of reverse voltage.

• The dc side consists of two capacitor stacks of the same size while the middle point is grounded. The objective of the dc capacitors is to store energy for the power flow control and reduce the voltage ripple on the dc side. Capacitor stack size depends on two main factors: the amount of energy to be stored in the device and the time rate of change of the energy to be transferred into or out of the storage device. This depends mainly on the peak power rating of the power conversion unit as in equation (1). For the proposed model a 10 ms is chosen as a time rate of energy transfer (τ) which is used in capacitance calculation of equation (2) where Sn is the nominal MVA [7].

$$W = \tau \cdot S_n = \frac{1}{2} C V_{dc}^2 \tag{1}$$

$$C = \frac{2\tau \cdot S_n}{V_{dc}^2} \tag{2}$$

### A. *Modelling of Voltage Source Converter (VSC):*

The dynamic model of a two-level sinusoidal Pulse-Width Modulation (SPWM) VSC in d-q synchronous reference frame is presented as discussed in the literature [8-10]. The two-level VSC shown in Fig. 2 represents both the on-shore converter which operates as inverter and the off-shore converter which operate as rectifier while the ac system represents either the grid or the WPP. The power flow between the ac system and the dc-link is bidirectional.

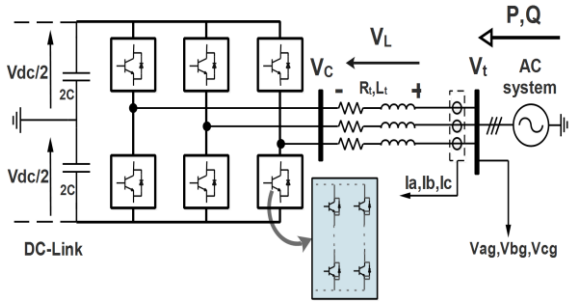


Fig. 2 Two-level Voltage Source Converter (VSC)

#### 1) *VSC in d-q synchronous reference frame:*

Considering that the power is transferred from the ac system to the dc-link through the phase reactor ($R_t$,$L_t$) shown in Fig. 2 which represents the sum of the total resistance and inductance of the $R_L$ filter and the transformer windings. The voltage drop across the phase reactor $V_L(t)$ is given in equation (3) where $V_t(t)$ is the three-phase ac system voltage and VC(t) is the converter output voltage. Applying voltage invariant Clark transformation in stationary reference frame, equation (4) is derived.

$$V_t(t) - V_C(t) = V_L(t) \tag{3}$$

$$V_{t\alpha\beta} - V_{C\alpha\beta} = R_C i_{\alpha\beta} + L_C \frac{di_{\alpha\beta}}{dt} \tag{4}$$

By applying the Park's transformation to (4) equation (5) is obtained where ω is the ac system frequency in rad/sec.

$$V_{tdq} - V_{Cdq} = R_C i_{dq} + \omega L_C i_{dq} + L_C \frac{di_{dq}}{dt} \tag{5}$$

The converter output voltage equations in the d-q synchronous reference frame can be written as:

$$V_{Cd} = V_{td} - R_C i_d - L_C \frac{di_d}{dt} + \omega L_C i_q \tag{6}$$

$$V_{Cq} = V_{tq} - R_C i_q - L_C \frac{di_q}{dt} - \omega L_C i_d \tag{7}$$

Where $V_{td}$ and $V_{tq}$ are the d-q ac system terminal voltages, $V_{Cd}$ and $V_{Cq}$ are the d-q converter voltages, and $i_d$ and $i_q$ are the d-q currents.

#### 2) *VSC* active and reactive power in d-q synchronous reference frame:

The apparent power S at the point of common coupling (PCC) in d-q reference frame is given by equation (8) where the sign (∗) represents the complex conjugation of the current vector.

$$S = \frac{3}{2} V_{tdq} i_{dq}^* = \frac{3}{2} (V_{td} + jV_{tq})(i_d - ji_q) \tag{8}$$

Hence active and reactive power of the VSC measured at the PCC (ac side) are given respectively by:

$$P = \frac{3}{2} (V_{td} i_d + V_{tq} i_q) \tag{9}$$

$$Q = \frac{3}{2} (V_{tq} i_d - V_{td} i_q) \tag{10}$$

### B. *DC-link Power:*

For a steady-state operation, active power exchange

at the ac side will be equal to the power exchange at the dc bus (neglecting the semiconductors losses) as in equations (11).

$$P_{dc} = P_{ac}$$
$$V_{dc} I_{dc} = \frac{3}{2}(V_{td} i_d + V_{tq} i_q) \quad (11)$$

Then, the DC current is given by:

$$I_{dc} = \frac{P_{ac}}{V_{dc}} = \frac{3(V_{td} i_d + V_{tq} i_q)}{2V_{dc}} \quad (12)$$

Which means that the converter at the dc side will be seen as a constant current source of magnitude Idc. Therefore, when ac system is connected to VSC, the d-q reference frame is used to make a fully decoupled linear control of active and reactive currents.

## 3. Control strategy

The control strategy of HVDC transmission systems mainly depends on the application [11]. In this section the grid synchronization process is analysed and the control strategy of the proposed model for both on-shore and off-shore converter stations are presented.

### *A. Grid Synchronization:*

In power converter interfacing renewable energy sources to the grid, the grid variables should be continuously monitored to ensure that the grid state is suitable for the correct operation of the power converter. There are several methods capable to detect the phase angle as discussed in [12]. The most commonly used method in three-phase systems is the synchronous frame Phase- Locked Loop (SF-PLL).

The block diagram of SF-PLL is illustrated in Fig. 3, where the three phase voltages are sensed and the instantaneous phase angle (θ) is detected by synchronizing the PLL rotating reference frame to the grid voltage vector.

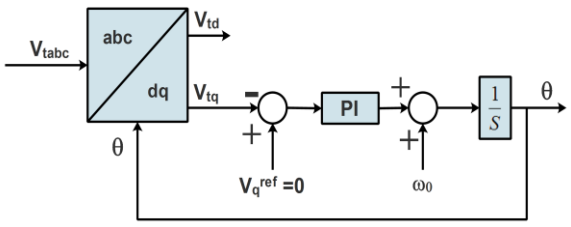


Fig. 3 Phase locked loop block diagram

The grid voltage has been chosen to be aligned with d-axis i.e. the q-axis voltage is zero while the d-axis voltage has the grid voltage magnitude. This is done by using a PI controller to force the quadrature axis to reach zero value. A feed-forward term ($\omega_o$) is introduced to improve the overall tracking performance of the PLL where (ωo) is the frequency of the grid. Finally, the frequency is integrated to obtain the grid voltage angle (θ).

### *B. On-shore converter station control:*

One of the advantages of VSC-HVDC is that it makes possible to independently control the active power and the reactive power. The active power depends on the power generated from the off-side that can be controlled either directly or by using a droop characteristics which called (DC droop control) [13]. The reactive power under normal operating condition is set to zero for a unity power factor operation. In some applications, the reactive power can be controlled to compensate for the reactive power demand or support the grid ac voltage when it drops under certain limits depending on each country grid code (e.g. Static synchronous compensator (STATCOM) [14]).

Recalling again equations (9) and (10) while the grid voltage is aligned into d-axis i.e. ($V_{td} = V_t, V_{tq} = 0$) equations of active and reactive power can be given by:

$$P = \frac{3}{2} V_{td} i_d \quad (13)$$

$$Q = -\frac{3}{2} V_{td} i_q \quad (14)$$

It is clear that the active and reactive power are controlled through the two-decoupled currents id and iq. The control loops of the on-shore converter station consist of two control loops, power and current loops as shown in Fig. 4. The outer loop (power loop) compares the reference values of active and reactive power ($P_r$, $Q_r$) to the measured values. The error is controlled using a proportional-integral (PI) controller which are the current references ($i_{dr}$, $i_{dr}$). The current references are compared with the actual currents which are controlled using a PI controller providing the reference voltage across the reactor.

The converter reference voltages ($V_{Cdr}$, $V_{Cqr}$) in dq-synchronous frame are transformed to abc- three phase voltages for PWM. The two terms $\omega_g L_g i_q$ and $\omega_g L_g i_d$ are used to compensate for the coupling between the d- and q axis.

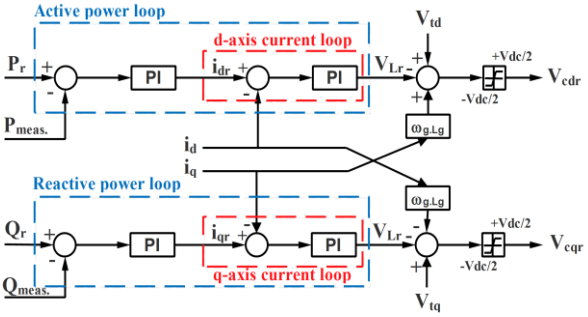


Fig. 4 On-shore station closed loop control system.

### *C. Off-shore converter station control:*

The off-shore converter control goal is to keep the dc-link voltage constant at its reference value. Consequently, the active power is controlled according to equation (13) by controlling the d-axis current. The reactive power is often set to zero for unity power factor operation.

The off-shore converter control loop consists of two control loops; the inner loop is a current regulator and the outer loop is a voltage regulator as shown in Fig. 5. The dc bus voltage is sensed and compared to the reference value then the error signal is regulated by a PI regulator. The output of the voltage regulator (the reference d-axis current) is compared to the measured d-axis current. Finally, the current error is regulated through a PI current regulator that gives the reference voltage across the reactor as mentioned before. The reactive power control consists of a current regulator to ensure that the q-axis current is set to zero.

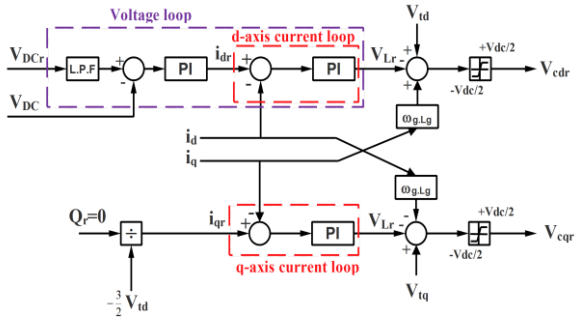


Fig. 5 Off-shore station closed loop control system.

## 4. Simulation Results

The behaviour of the VSC-HVDC transmission system has been analysed in different conditions. The system was simulated using MATLAB/SIMULINK package. The IGBT modules were simplified as one IGBT module for the top and another for the bottom half of each leg. The capacitor bank for the dc-link was simplified to one capacitor for the positive and negative dc-link voltage. The switching frequency has been chosen as 2.5 kHz. Two cases were analysed in order to evaluate the behaviour of the system as follow:

### *A. CASE1: Sending only active power (P):*

For wind power applications, the active power exchange is unidirectional, the power can be transferred from the off-shore to the grid side. At t=0.2 s the reference active power sent to the grid was set to 200 MW i.e. (0.67 p.u) till 0.4 the reference was increased into 1 p.u. At t=0.6 s the reference active power has been decreased again to 0.67 p.u and finally to zero. The reference reactive power was set to zero for unity power factor operation. Fig. 6.a shows the reference and measured active and reactive power injected to the grid. As shown in figure, the measured values track the references having 20 ms settling time with zero-steady state error. By increasing the power demand, the current increases similarly as shown in Fig. 6.b. Fig. 6.c shows the effect of the dc-link voltage under different power conditions. Points from 1 and 2 shows that with the increase of the active power demand the dc-link voltage decreases slightly. Consequently, the voltage controller operates to bring the dc voltage back again to its reference value. Points 3 and 4 occurred when the active power demand decreased which results in a slight increase of the dc-link voltage. The dc voltage returned to its reference by the voltage controller action.

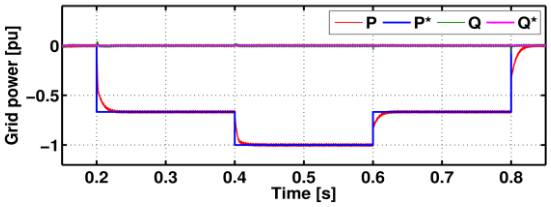


(a) Reference and actual value of the injected active power

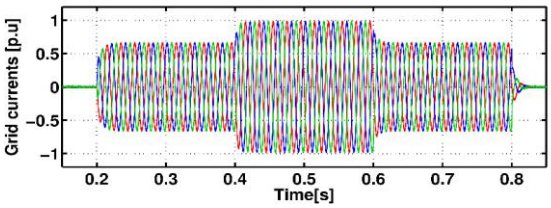


(b) Grid current under variation of demand power

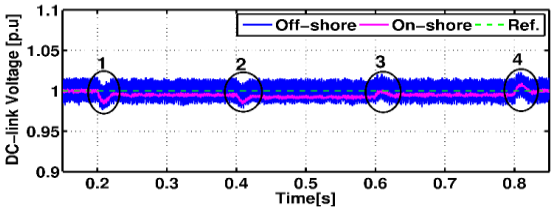


(c) dc-link voltage under variation of the active power demand

Fig. 6 Case1: Active power injected into the grid

The grid voltage and current of phase A shown in Fig. 7. The current is 180o apart from the grid voltage which means the current is negative (the direction from the inverter to the grid) with no phase angle difference. As seen, the current has increased to 1 p.u at 0.4 s to deliver the rated active power demand.

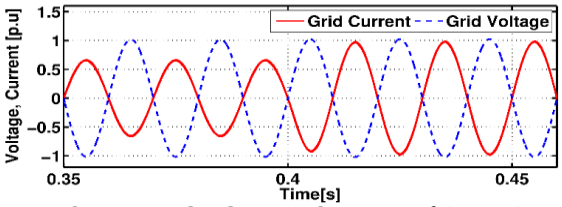


Fig. 7 Phase A grid voltage and current of (case:1).

### *B. CASE2: Sending only reactive power (Q):*

The behaviour of the VSC-HVDC system was analysed while sending only reactive power with zero active power injection. In order to evaluate the controller performance of the inverter, the reactive power was set to -100 MVAR i.e. (0.33 p.u) at t=0.2 s then changed to +0.33 p.u at t=0.4s, -0.33 p.u again at t=0.6s and finally to zero at t=0.5 s. The active power was set to be zero for evaluation of reactive component only. Fig. 8.a shows a good performance of the

controller. The measured power followed the reference having 20 ms of settling time with zero-steady state error and no overshoot in both directions.

The three phase grid currents as in Fig. 8.b show the dynamic behavior of currents while changing direction of reactive power flow from negative (sending) to positive (receiving). From Fig. 8.c, the dc-link voltage is not affected by the reactive power exchange.

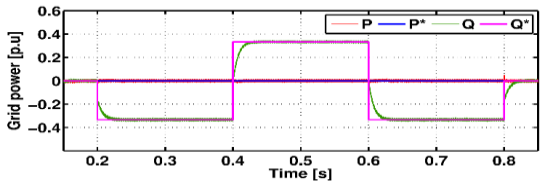


(a) Reference and actual value.

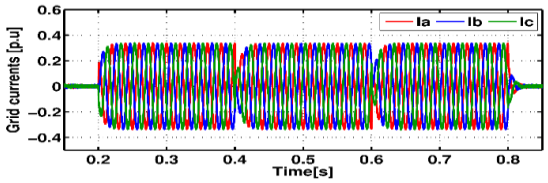


(b) Grid current under reactive power reversal.

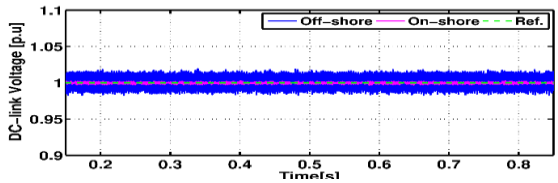


(c) dc-link voltage

Fig. 8 Case2: Reactive power injected into the grid.

Finally, Figure 9 shows the phase shift between the grid current and voltage during sending and receiving reactive power. It is clear that in the first period while sending reactive power (-Q), the grid current lead the grid voltage by 90° as in Fig. 9.a. While receiving the reactive power (+Q) the grid current lags the grid voltage by 90° as in Fig. 9.b.

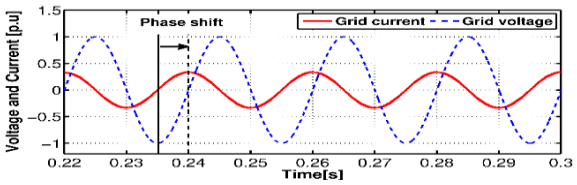


(a) current leads voltage by 90°

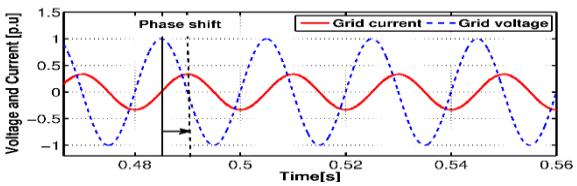


(b) Grid current lags voltage by 90°

Fig. 9 Grid current of phase A under changing reactive power direction.

## 5. Experimental setup

The behavior of the on-shore inverter side was verified experimentally through a small- scale inverter supplied by a fixed dc source. The three-phase inverter was connected to a virtual grid i.e. the grid voltage was sensed to obtain the grid angle but the inverter output was connected to a three-phase RL load. The voltages and currents of phase A and B were sensed then sent to the controller board as shown in Fig. 10. The controller board consists of three stages as following:

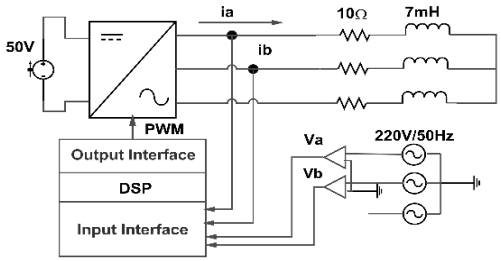


Fig. 10 Three phase inverter connected to a virtual grid.

### A. *Input interface:*

The received signals from the current and voltage sensors were filtered from high- frequency noise produced by the switching of the IGBTs then adapted to take values between 0 to 3V dc.

### B. *Output interface:*

The output interface circuit is the drive circuit which adapts the Pulse-Width Modulation (PWM) output signals of the controller to the operating voltage of the IGBT drivers. The MTL-CBI0010N12IXFE Guash power stack requires +15V dc gate signals.

### C. *Digital Signal Processor (DSP):*

The output signals from the input interface were connected to the A/D module of the DSP TMS320F28335. The potentiometers included in the board were used to set the active and reactive power references. The overall hardware implementation of the three-phase inverter connected to a virtual grid is shown in Fig. 11.

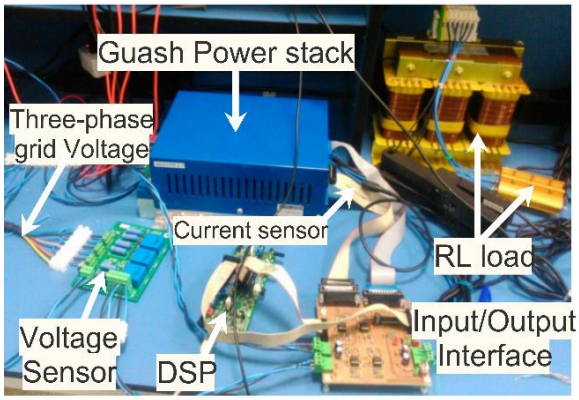


Fig. 11 Hardware implementation of the system.

## 6. Experimental Results

The inverter output was connected to an RL load while the grid angle was obtained by sensing the grid voltage. As a result, the current direction has to be the inverse of the simulation results as shown in Fig. 14. For the first case only the active power was applied to the controller which results of having the current in phase with the grid voltage as seen in Fig. 12.(a). While in the second case the system with setting a reference of positive and negative reactive power. The current with the grid voltage waveforms while sending (+Q) and (-Q) are shown in Fig. 12.(b) and Fig. 12.(c) respectively.

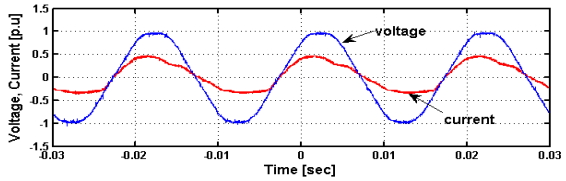


(a) Current in phase with the voltage with active power injection.

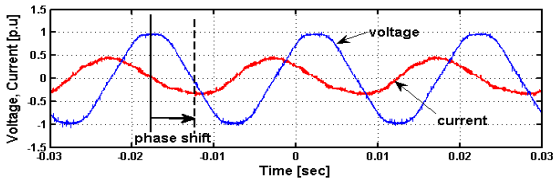


(b) Current leads voltage by 90° with reactive power injection.

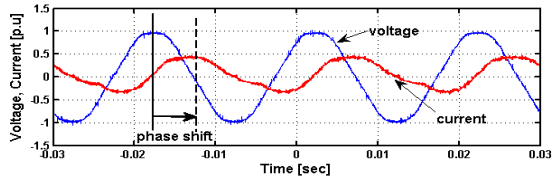


(c) Current lags voltage by 90° with reactive power absorption.

Fig. 12 Phase A current and voltage measured under operating conditions.

## 7. Conclusions

The paper studies the integration performance of off-shore wind power plants through the HVDC-VSC based transmission. In addition, the vector control of the grid side converter was implemented showing that the experimental and simulation results were matched for independently control of active and reactive power. Consequently, the inverter reactive power can be controlled to compensate the reactive power change at the PCC. Which in returns helps to mitigate the grid voltage disturbances to keep grid voltage within limits.

The system implementation can be used to study the factors affecting on the grid integration of renewable energy systems using VSCs. Grid impedance, grid angle and phase looked loop are most common factors affecting on the integration process that are still an interesting topic under investigation.

## Appendix

Table 1: System Parameters

| Parameter | Value |
|---|---|
| Reactor resistance, $R_g/R_{wf}$ | 0.8 Ω |
| Reactor inductance, $L_g/L_{wf}$ | 1 mH |
| DC-link Capacitor, C | 300 µF |
| DC-cable resistance, $R_{dc}$ | 0.01 Ω/Km |
| DC-cable inductance, $L_{dc}$ | 0.01 mH/Km |


## Acknowledgment

This work is done in University of Oviedo in cooperation with Port Said University through Erasmus Mundus Mobility Fund "Medastar" 2014-2015 program.


## References


1. The Global Wind Energy Council., 'GWEC wind 2014 report', 2014.
2. Flourentzou N, et al.: "VSC-based HVDC power transmission systems: An overview", IEEE Transactions in Power Electronics, Vol. 24, No. 3, 2009, pp. 592-602.
3. Arrillaga J, et al.: "Flexible power transmission: the HVDC options" (John Wiley & Sons; 2007 Sep 27).
4. Anaya-Lara O, et al, "Offshore Wind Energy Generation: Control, Protection, and Integration to Electrical Systems" (John Wiley & Sons; 2014 Mar 26).
5. Chaudhuri N, et al, "Multi-terminal Direct-current Grids: Modeling, Analysis, and Control" (John Wiley & Sons; 2014 Sep 9).
6. Arritt RF and Dugan RC.: "Distributed generation interconnection transformer and grounding selection", In Power and Energy Society General Meeting, Jul 2008, pp. 1-7.
7. Kalitjuka T.: "Control of Voltage Source Converters for Power System Applications". MSc thesis, NTNU, Norway, 2011.
8. Teodorescu R, et al.: "Grid converters for photovoltaic and wind power systems" (John Wiley & Sons; 2011).
9. Mulugeta T.: "Control, Dynamics and Operation of Multi-terminal VSC-HVDC Transmission Systems". PhD thesis, NTNU, Norway, 2012.
10. Wu B, et al.: "Power conversion and control of wind energy systems" (John Wiley & Sons; 2011 Aug 9).
11. J. Pan, et al, "AC Grid with Embedded VSC-HVDC for Secure and Efficient Power Delivery", Energy 2030 Conference, IEEE, Atlanta, GA, 2008, pp. 1-6.
12. Guo XQ, Wu WY and Gu HR.: "Phase locked loop and synchronization methods for grid interfaced converters: a review", PRZEGLĄD ELEKTROTECHNICZNY, Vol. 87, No. 4, Jan 2011, pp. 182-187.
13. J. Beerten and R. Belmans: "Modeling and Control of Multi-Terminal VSC HVDC Systems", Energy Procedia, Vol. 24, 2012, pp. 123-130.
14. Li S, Xu L and Haskew TA.: "Control of VSC-based STATCOM using conventional and direct- current vector control strategies", International Journal of Electrical Power & Energy Systems, Vol. 45, No. 1, Feb 2013, pp. 175-86.